



HAL
open science

Indium Tin Oxide Microsystem for Electrochemical Detection of Exocytosis of Migratory Dendritic Cells

Xiaoqing Liu, Marine Bretou, Ana-Maria Lennon-Duménil, Frédéric Lemaître, Manon Guille-Collignon

► **To cite this version:**

Xiaoqing Liu, Marine Bretou, Ana-Maria Lennon-Duménil, Frédéric Lemaître, Manon Guille-Collignon. Indium Tin Oxide Microsystem for Electrochemical Detection of Exocytosis of Migratory Dendritic Cells. *Electroanalysis*, 2016, ESEAC Conference 2016, 29 (1), pp.197-202. 10.1002/elan.201600360 . hal-01520269

HAL Id: hal-01520269

<https://hal.sorbonne-universite.fr/hal-01520269v1>

Submitted on 10 May 2017

HAL is a multi-disciplinary open access archive for the deposit and dissemination of scientific research documents, whether they are published or not. The documents may come from teaching and research institutions in France or abroad, or from public or private research centers.

L'archive ouverte pluridisciplinaire **HAL**, est destinée au dépôt et à la diffusion de documents scientifiques de niveau recherche, publiés ou non, émanant des établissements d'enseignement et de recherche français ou étrangers, des laboratoires publics ou privés.

Indium Tin Oxide Microsystem for Electrochemical Detection of Exocytosis of Migratory Dendritic Cells

Xiaoqing Liu,^{a,b} Marine Bretou,^c Ana-Maria Lennon-Duménil,^c Frédéric Lemaître,^{a,b} Manon Guille-Collignon^{a,b*}

^a Ecole normale supérieure, PSL Research University, UPMC Univ Paris 06, CNRS, Département de Chimie, PASTEUR, 24, rue Lhomond, 75005 Paris, France

^b Sorbonne Universités, UPMC Univ Paris 06, ENS, CNRS, PASTEUR, 75005 Paris, France

^c INSERM U932, Inst Curie, 12, rue Lhomond, 75005 Paris, France

* e-mail: manon.guille@ens.fr

Abstract

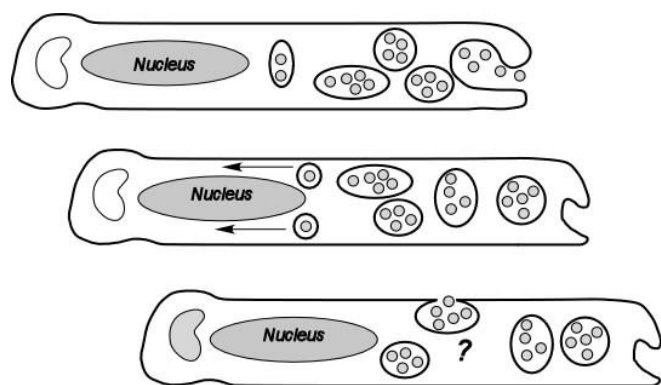
The design, fabrication and test of an indium tin oxide (ITO) microdevice to investigate exocytotic behaviors of migratory dendritic cells (DCs) in confined three-dimensional environment were reported in this work. Indeed, immature DCs were able to migrate into micro-fabricated biocompatible polydimethylsiloxane (PDMS) channels that mimic their natural constrained environment of tissues for patrolling in search of danger associated antigens through an endocytotic process called macropinocytosis. In order to coordinate membrane trafficking and prevent cell volume increment, DCs will release part of their contents back to the extracellular medium while migrating. Through electrochemical measurements, we demonstrated that exocytotic events of migratory DCs could be monitored by our ITO microdevice. In addition, the transparency of ITO electrode should facilitate future combining assays of exocytosis with other fluorescence-based measurements of cell physiology.

Keywords: Electrochemical detection; Exocytosis; ITO microsystem; Dendritic cells; Cell migration

Dendritic cells (DCs), the most potent antigen (AG) presenting cells, are the sentinels of the immune system.^[1-3] They effectively patrol peripheral tissues in search of danger associated AG through a biological phenomenon called “macropinocytosis”. This process constitutes the first step of the adaptive immune response and significantly relies on specific DCs properties, including their high endocytic capacity^[4, 5] as well as their efficient motility^[6] in confined three-dimensional (3D) environments. Macropinocytosis represents a distinct pathway of endocytosis in mammalian cells (Scheme 1).^[7-9] It includes the uptake of cargo from the extracellular medium by macropinosomes, the preservation of the surface membrane area, and the regulation of membrane traffic along the intracellular pathway. Interestingly, previous study^[7] shows that

macropinosome traffic is not unidirectional (endocytic), but bidirectional (endocytic and exocytotic), indicating that DCs macropinocytosis is accompanied by exocytotic events. Recently, high resolution time-lapse imaging confirms that exocytosis is taking place when DCs migrate in the confined 3D microchannels.^[10] Such secretory events might favor matrix remodeling and membrane recycling required for cell migration. Moreover, this exocytotic process taking place in DCs plays an important role in proper cell communication/activation, and need to be tightly controlled in order to allow either an efficient clearance of pathogens, or the maintenance of immune homeostasis. Characterization of exocytosis of migratory DCs is thus significant to better understand the cellular trafficking in 3D-confinement. In this context, secretion coupled to cell

migration has been poorly addressed. This is why we considered to use amperometry in 3D-confined microchannels that mimics the confined environment in which DCs migrate. Indeed, amperometry is a routine analytical technique for quantitative, real-time monitoring of exocytosis at single cell level.^[11-13] In general, a microelectrode is positioned in the close vicinity of a target cell during amperometric measurement, either on the top or at the bottom, and a constant potential is applied to the working electrode at which electrochemical biomolecules (mainly catecholamines) released during exocytosis could be oxidized. As a consequence, the exocytotic fluxes are depicted as a series of amperometric current spikes and each single spike results from an individual exocytotic event.^[14] The frequency and shapes of amperometric spikes elucidate particular information about the dynamics of the release process while their integrals give the exact quantity of electroactive molecules released. Different microelectrodes (carbon fiber^[11, 14-16], Au^[17], Pt^[18]...) have been employed for amperometric detection of electroactive molecules discharged from individual vesicle during exocytosis. Among them, indium tin oxide (ITO) microelectrodes appear to be a good choice due to their excellent optical transparency, high electrical conductivity as well as their appropriate electrochemical working window for the electroanalysis of biomessengers. Our group and others have been developing microchips based on transparent ITO microelectrodes on a glass substrate in order to facilitate higher throughput measurements of exocytosis as well as to enable fluorescent measurements that are not possible with usual carbon-fiber electrodes.^[19-23]



Scheme 1. Schematic view of macropinocytosis process. Top : Formation of macropinosomes at the front of the migrating dendritic cell while it is moving. Middle : Antigen presentation towards the back of the cell, behind the nucleus. Vesicles undergo series of morphological changes to concentrate the internalized antigen. Bottom: Possible exocytotic event towards the extracellular medium so as to achieve the membrane retrieval and excessive fluid discharge.

To the best of our knowledge, there have been so far few researches focusing on studies of exocytotic behaviors of DCs. In 2006, by means of fluorescent microscopy, macropinocytosis of DCs was found to be a regulated coordination of endocytic and exocytotic membrane traffic events.^[7] The membrane release of serotonin from DCs upon ATP stimulation was also confirmed by amperometric measurement with carbon fiber microelectrode.^[24] However, these studies have been mainly performed *ex vivo* on flat two-dimensional (2D) surfaces and such substrates rarely apply to *in vivo* cell migration, which mainly occurs in 3D confined environment. Exocytotic behaviors of migratory DCs in 3D confinement, as *in vivo*, were investigated in this article by designing and fabrication of a PDMS microchannels/ITO microsystem (Fig.1 (A)) allowing simultaneous observation of cells and amperometric detection of exocytosis as described herein. (The details concerning ITO microdevice assembly are shown as supporting information in Fig.S-1)

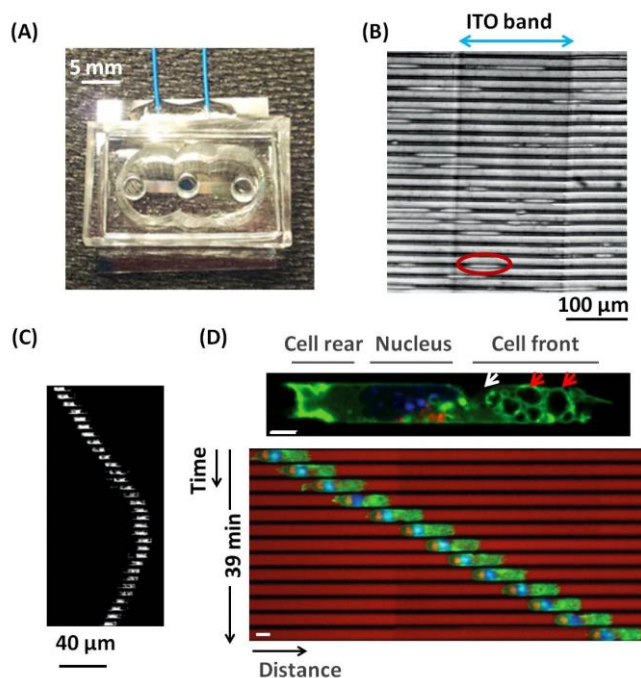


Figure 1. (A) ITO microdevice for amperometric detection; (B) DCs migrating to the fibronectin coated ITO/glass substrate; the blue double headed arrow depicts the position of the transparent ITO microelectrode and the red ellipse indicates the single migratory DC lying on ITO band; (C) A typical example of an individual DC migrating in 4- μ m width*5- μ m height fibronectin-coated microchannels. Sequential images were processed to remove the channels so that only the cells are visible (white). Temporal sequences were put one below the other (Magnification 10 \times , the interval between two images is 2 min, scale bar 40 μ m). (D) Top: A representative Life-act-GFP DC in 8- μ m width*5- μ m height fibronectin-coated

microchannels: the nucleus was stained with Hoechst (in blue); lysosomes in red were tagged with WGA-AF647 and macropinosomes of the migrating DC were indicated by the white arrows at the cell front (Magnification 60 \times); Sequential images of the life-act-GFP DC migrating in microchannels filled with OVA AF-647 (in red). Temporal sequences were put one below the other (Magnification 20 \times , one image every 3 min, scale bar: 5 μm). DC was able to internalize the OVA-647 in the channels and it was finally accumulated into the lysosomes at the cell rear during migration. Several events of secretions might be envisioned for a single DC.^[24] For instance, a vesicle formed at the cell front could be exocytosed (indicated by the red arrow in the top image).

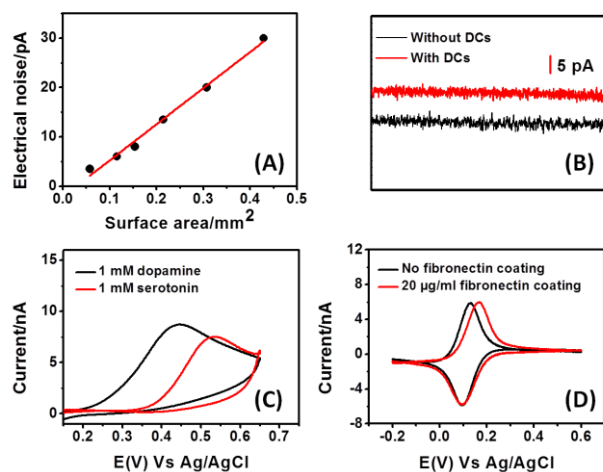
3D-confined microchannels made of PDMS, a biocompatible silicone elastomer, have been demonstrated to be able to induce DCs to move inside the microchannels at speeds similar to those observed *in vivo*.^[6, 10, 25, 26] In our case, the transparent property of the bottom ITO-embedded glass slide allowed us to observe DCs' behaviors through high-resolution microscopy. Additionally, multiple parallel channels in each device (around 80 channels per chamber), enabled an easy recording of many cells' behaviors at low magnification. As shown in Fig.1 (B), after overnight incubation, DCs previously loaded into the entry plug of the ITO microdevice spontaneously entered into PDMS microchannels and were able to move across the ITO electrode, without any mechanical or chemical stimulation. By tracking DCs' migration along PDMS microchannels with time-lapse imaging, we noticed that not all the cells acted at the same way inside the microchannels (see movie 1 shown in supporting information). Firstly, there were big differences of cell sizes; secondly, most cells underwent important speed fluctuations during motion, resulting in different migration distances; finally, some cells showed changes in direction during migration (Fig.1 (C)). However, after overnight incubation, we always saw DCs moving on ITO electrode.

Figure 2. (A) Measurements of the electrical noise in PBS (pH=7.4) at a constant potential value ($E=+650$ mV vs. Ag/AgCl) as a function of electrodes dimensions ($y=70x-2$, $R^2=0.948$); (B) Electrical noise of ITO microelectrode with and without DCs and its dimension is of 200 μm by 320 μm ; (C) Cyclic voltammograms of 1 mM serotonin and 1 mM dopamine in PBS solution (pH=7.4) respectively, scan rate 20 mV/s. (D) Cyclic voltammograms of 100 μM $\text{K}_3\text{Fe}(\text{CN})_6$ in PBS (pH=7.4) on ITO electrode with and without fibronectin treatment, scan rate 20 mV/s.

As shown in Fig.1(D), by staining the different compartments of DCs with specific dyes, we found that while migrating along the microchannels, DCs could form lots of macropinosomes (as indicated by the white arrows in Fig.1(D)) in front of the nucleus to sample the microenvironment so as to take up extracellular antigens and the internalized antigens were accumulated in lysosomes at the cell rear (Fig.1(D)). We thus believe that migrating DCs are able to expel part of their contents to the extracellular space so as to achieve the coordination of endocytic and exocytotic membrane trafficking. That is, exocytotic events are properly taking place during migration. Previous studies have shown that DCs are able to not only accumulate neurotransmitters but also synthesize, store and degrade them. Since neurotransmitters play important roles in immune response of DCs,^[27, 28] we try to figure out if there are electroactive neurotransmitters, like serotonin or dopamine, expelled by DCs during migration with amperometric detection.^[24, 29-31] This is different from what have been shown before in the literature in the way that secretion is monitored here while the DCs are confined in 3D microdevices and are migrating into the ITO microsystem channels assembly.

Fig.2 (A) presents the relationship between the current noise and the surface area of ITO working electrode of which the band widths varied from 200 μm to 1000 μm . Globally the line depicts a good linear fit with a slope of 0.07 $\text{fA}/\mu\text{m}^2$. Moreover, the best electrical properties were obtained from 200 μm ITO band with minimum surface area of 0.06 mm^2 , with a rms noise of typically 2 to 4 pA, which is consistent with our previous work based on ITO microelectrodes.^[22] We also compared the current noises obtained from ITO microelectrodes with and without DCs. As illustrated in Fig.2 (B), migratory DCs adjacent to ITO electrodes didn't increase the background noise for amperometric recordings. All measurements were performed in PBS (phosphate buffer saline) solution and no obvious difference was seen for the two parallel ITO microelectrodes in the same microdevice.

Fig.2 (C) shows cyclic voltammograms of two well-known neurotransmitters (1 mM serotonin and 1 mM dopamine) inside the 3D-confined microchannels



collected on ITO microelectrode at a scan rate of 20 mV/s. We can see that dopamine started to be oxidized at about +200 mV while the oxidation of serotonin occurred at +400 mV, and their oxidation peaks were located at around +450 mV and +550 mV, respectively. According to the results mentioned above, our ITO microdevice is adequate from an electrochemical point of view for amperometric detection of these electroactive neurotransmitters release. Therefore, in the following experiments, we applied a potential of +650 mV to track neurotransmitter release from DCs on ITO electrode by amperometric measurement, this value being identical with the one we used to detect serotonin discharged from cells by carbon-fiber and ITO electrodes in previous references. [22, 23, 32]

In our microdevice, the bottom surface for DCs' migration is composed by both ITO and glass, showing inhomogeneity, further surface treatment is thus necessary to let DCs adhere and spread in PDMS microchannels. For the sake of creating a homogenization of the whole surface, we pre-coated the microchannels with 20 $\mu\text{g}/\text{mL}$ fibronectin solution for one hour. To investigate whether electrochemical properties of ITO electrodes were affected by fibronectin treatment, we compared cyclic voltammogram of a well characterized redox mediator $\text{K}_3\text{Fe}(\text{CN})_6$ (100 μM) acquired on naked ITO microelectrode with that obtained from 20 $\mu\text{g}/\text{mL}$ -fibronectin precoated ITO band. As shown in Fig.2 (B), besides the slightly shift of the oxidation peak, fibronectin coating did not alter the electrochemical detection at ITO microelectrodes.

In our 3D-confined PDMS microchannels that mimic the natural constrained environment of tissues, DCs were able to migrate through the ITO microelectrode (Fig.1(B)). Previous study shows that for migrating DCs, exocytosis was taking place so as to empty part of the ingested fluid as well as to recycle the internalized membrane during macropinocytosis (Fig.1(D)).^[10] In this present work, based on ITO microelectrode, we tried to investigate the spontaneous exocytotic events of migratory DCs by amperometric detection, which provides the accurate amount of released biomolecules and precise kinetic characteristics with high sensitivity and sub-millisecond temporal resolution.

We applied a +650 mV constant potential at the ITO electrode vs. Ag/AgCl and recorded the current as a function of time. The exocytotic release trace from migratory DCs in 3D-confined PDMS microchannels thus appeared as a succession of individual, well separated amperometric spikes, as presented in Fig.3 (A).

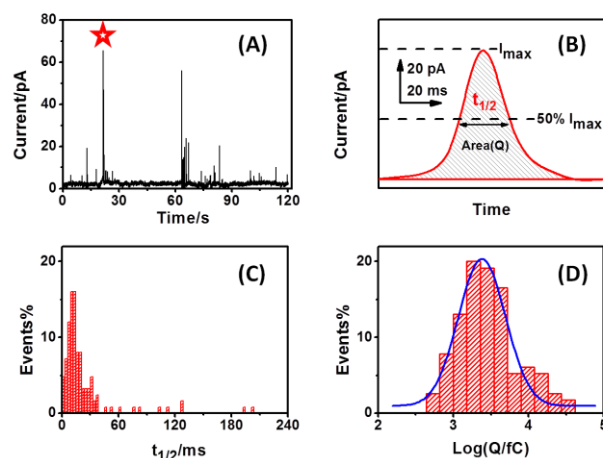


Figure 3. (A) Representative amperometric trace monitored on the 3D-confined ITO microdevice from migratory DCs; (B) A typical amperometric spike extracted from amperometric trace (indicated by the red star); (C) Histogram of half-height width ($t_{1/2}$); (D) Statistical logarithmic distributions ($y = 0.2e^{-5.6(x-3.4)^2}$, $R^2 = 0.932$) of the charge Q obtained for each exocytotic event electrochemically detected on the 3D-confined ITO microdevice for DCs.

At a potential at the foot of the oxidation waves of dopamine or serotonin (see Fig.2 (C), respectively, 100 and 300 mV vs. Ag/AgCl, no spikes were detected (data not shown). The current spikes suggested electroactive biomolecules were discharged by migratory DCs and then immediately oxidized at ITO surface, confirming the viewpoint that macropinocytosis of migratory DCs is accompanied by exocytotic events, resulting in the coordination of endocytic and exocytotic membrane trafficking. It is important to note that this secretion is detected in the absence of any stimulation/secretagogue nor prior loading of the cells with any neurotransmitter or electroactive molecule, pointing out the facts that the DCs have endogenous electroactive neurotransmitters^[28] and that the spontaneous secretion is probably triggered by confinement. Indeed the same experiments performed in Petri dishes with the technique of carbon fiber microelectrodes used by amperometry showed no secretion in the absence of stimulation or prior loading of the cells (data not shown).

Fig.3(B) displays a typical single oxidative spike on expanded time scale extracted from Fig.3(A), which is corresponding to an individual exocytotic event. In amperometric measurement, maximum current amplitude I_{max} (pA), half-height width $t_{1/2}$ (ms) and area Q (pC) are typical characteristics for a single spike analysis. Note that I_{max} represents the maximum release flux, $t_{1/2}$ is defined as the time interval where current amplitude exceeds 50% of I_{max} while the integral charge Q was employed to calculate the precise release amount on the

base of Faraday's law. For migratory DCs, we analyzed the results from a total of 125 events with a wide range of amplitudes varying from 5 to 120 pA (mean value, 21.9 ± 3.4 pA) and histograms of $t_{1/2}$ and integral Q were presented separately in Fig.3(C) and Fig.3(D). The distribution of $t_{1/2}$ values shows a half-height width of a few milliseconds, with a mean value of 25.05 ± 3.44 ms and the mean Q value is 0.74 ± 0.16 pC. However, larger, more irregularly shaped events also occurred (see Fig.S-2 shown in supporting information). These spikes may come from sites further from ITO microelectrode or represent multiple releases or another type/size of vesicles.

We have designed and manufactured an effective 3D-confined ITO/PDMS microdevice which allows simultaneously cell observation and amperometric measurement of exocytosis from migratory DCs. The phenomenon that macropinocytosis of migratory DCs is accompanied by exocytotic events was monitored by amperometric detection. We propose that our experiments will identify specific modes of exocytosis and will display the mutual interaction of endocytic and exocytotic trafficking of DCs as well as will quantitatively analyzing exocytosis during cell migration. In addition, further optimization of our microdevice based on transparent ITO microelectrode should facilitate future real-time combining assays of DCs' exocytotic behaviors with other fluorescence technology.^[23, 33, 34] By doing so, correlations between place (on the DC surface, rear or front) or size of vesicles (lysosomes, macropinosomes etc...) and quantitative parameters of secretion could be drawn.

Experimental

ITO microelectrodes were manufactured by photolithographic process and acidic wet etching (see Fig.S-1(A) shown in supporting information). A thin film of ITO (90% In_2O_3 /10% SnO_2 ; 150 nm thickness; ACM, Villiers Saint Frédéric, France) was previously sputtered onto optical glass slides (22 mm \times 22 mm \times 0.13 mm) in order to afford a material of low electrical resistance (≤ 20 ohms per square) and transparency. To be specific, firstly, an insulating photoresist (AZ 9260, Clariant GmbH, Germany) was patterned onto the ITO/glass slides by the following steps: (a) spin-coating (b), prebaking on a hotplate at 110°C, exposure to UV light through a specific mask design (c) and development (AZ 400K+ H_2O) (d). Then, the ITO with no "photoresist protective layer" was chemically etched by commercial HCl solution and the photoresist remaining on ITO band was removed with acetone. This 'wet etching' step left

two identical ITO microelectrodes of about 200- μm width respectively on the glass slide.

Biocompatible PDMS microchannels with the inlet and outlet ports were prepared as previously described.^[25, 26] In brief, microchannels were fabricated in PDMS using rapid prototyping and soft lithography. As a result, for each PDMS chamber (see Fig.S-1(B) shown in supporting information), multiple microchannels are run in parallel which makes it suitable for multiple cells observation. Moreover, we fixed a homemade PDMS gasket with diameter of 1.5 cm onto the top of the PDMS microchannels so as to hold the culture medium, making the chamber an appropriate environment for cells ((see Fig.S-1(C) shown in supporting information)). PDMS chamber and the ITO-embedded glass slide were then activated in a plasma cleaner (PDC-32G Harrick) for 1 min at 400 mTorr and were stuck together. One hour incubation in 60 °C oven was used to strengthen the binding. The upper surface of the microchip was then activated by plasma treatment for 2 min at 400 mTorr to produce hydrophilic inlet which enabled 20 $\mu\text{g}/\text{mL}$ fibronectin (fibronectin from bovine plasma 0.1% solution) to fill into the microchannels. After one hour coating at room temperature, the microchip was rinsed 3 times with PBS. The system could be used immediately or stored up to 3 days at +4 °C. Before loading cells, microchannels were washed twice with cell culture medium and kept in the incubator while collecting cells.

Amperometric detection of exocytosis at ITO microelectrodes was carried out using a picoamperometer (model AMU-130, Radiometer Analytical Instruments, Copenhagen, DK) at a constant potential $E = + 650$ mV vs. a silver/silver chloride reference electrode (Ag/AgCl, a 1-mm diameter wire). The time course of the amperometric current was monitored (output digitized at 40 kHz) and stored on a computer (Latitude D600, Dell) through a D/A converter (Powerlab 4SP, AD Instruments) and its software interface (Chart version 4.2 for Windows, ADInstruments). The significative parameters of an amperometric spike are the maximum oxidation current I_{max} (pA), the half-height width $t_{1/2}$ (ms) and the total electrical charge Q (pC). All the values are presented as the mean \pm s.e.m. (standard error of the mean = standard deviation/ \sqrt{n} , where n is the number of spikes analyzed). Voltammetric analyses were performed with an EA162 Picostat (eDAQ, Australia) through an e-corder 401 system associated with EChem software. The reference electrode was also Ag/AgCl.

Acknowledgements (optional)

This work has been supported in part by CNRS (UMR 8640), Ecole Normale Supérieure (PSL Research University), French Ministry of Research and Université Pierre & Marie Curie Paris 6 (Sorbonne Universités). M.

References

- [1] M. F. Lipscomb, B. J. Masten, *Physiol. Rev.* **2002**, *82*, 97-130.
- [2] J. Banchereau, R. M. Steinman, *Nature* **1998**, *392*, 245-252.
- [3] J. Banchereau, F. Briere, C. Caux, J. Davoust, S. Lebecque, Y. T. Liu, B. Pulendran, K. Palucka, *Annu. Rev. Immunol.* **2000**, *18*, 767-+.
- [4] A. E. Morelli, A. T. Larregina, W. J. Shufesky, M. L. G. Sullivan, D. B. Stolz, G. D. Papworth, A. F. Zahorchak, A. J. Logar, Z. L. Wang, S. C. Watkins, L. D. Faló, A. W. Thomson, *Blood* **2004**, *104*, 3257-3266.
- [5] W. S. Garrett, L. M. Chen, R. Kroschewski, M. Ebersold, S. Turley, S. Trombetta, J. E. Galan, I. Mellman, *Cell* **2000**, *102*, 325-334.
- [6] M. L. Heuze, P. Vargas, M. Chabaud, M. Le Berre, Y.-J. Liu, O. Collin, P. Solanes, R. Voituriez, M. Piel, A.-M. Lennon-Dumenil, *Immunol. Rev.* **2013**, *256*, 240-254.
- [7] S. Falcone, E. Cocucci, P. Podini, T. Kirchhausen, E. Clementi, J. Meldolesi, *Journal of Cell Science* **2006**, *119*, 4758-4769.
- [8] A. T. Jones, *Journal of Cellular and Molecular Medicine* **2007**, *11*, 670-684.
- [9] M. C. Kerr, R. D. Teasdale, *Traffic* **2009**, *10*, 364-371.
- [10] M. Chabaud, M. L. Heuzé, M. Bretou, P. Vargas, P. Maiuri, P. Solanes, M. Maurin, E. Terriac, M. Le Berre, D. Lankar, T. Piolot, R. S. Adelstein, Y. Zhang, M. Sixt, J. Jacobelli, O. Bénichou, R. Voituriez, M. Piel, A.-M. Lennon-Duménil, *Nature Communications* **2015**, *6*, 7526.
- [11] C. Amatore, S. Arbault, M. Guille, F. Lemaître, *Chemical Reviews* **2008**, *108*, 2585-2621.
- [12] A.-S. Cans, A. G. Ewing, *J. Solid State Electrochem.* **2011**, *15*, 1437-1450.
- [13] F. Lemaître, M. G. Collignon, C. Amatore, *Electrochimica Acta* **2014**, *140*, 457-466.
- [14] R. M. Wightman, J. A. Jankowski, R. T. Kennedy, K. T. Kawagoe, T. J. Schroeder, D. J. Leszczyszyn, J. A. Near, E. J. Diliberto, O. H. Viveros, *Proceedings of the National Academy of Sciences of the United States of America* **1991**, *88*, 10754-10758.
- [15] M. L. Huffman, B. J. Venton, *Analyst* **2009**, *134*, 18-24.
- [16] T. J. Schroeder, J. A. Jankowski, K. T. Kawagoe, R. M. Wightman, C. Lefrou, C. Amatore, *Analytical Chemistry* **1992**, *64*, 3077-3083.
- [17] P. Chen, B. Xu, N. Tokranova, X. J. Feng, J. Castracane, K. D. Gillis, *Analytical Chemistry* **2003**, *75*, 518-524.
- [18] A. F. Dias, G. Dernick, V. Valero, M. G. Yong, C. D. James, H. G. Craighead, M. Lindau, *Nanotechnology* **2002**, *13*, 285-289.
- [19] X. H. Chen, Y. F. Gao, M. Hossain, S. Gangopadhyay, K. D. Gillis, *Lab Chip* **2008**, *8*, 161-169.
- [20] C. L. Gao, X. H. Sun, K. D. Gillis, *Biomed. Microdevices* **2013**, *15*, 445-451.
- [21] X. H. Sun, K. D. Gillis, *Analytical Chemistry* **2006**, *78*, 2521-2525.
- [22] A. Meunier, R. Fulcrand, F. Darchen, M. Guille Collignon, F. Lemaître, C. Amatore, *Biophysical Chemistry* **2012**, *162*, 14-21.
- [23] A. Meunier, O. Jouannot, R. Fulcrand, I. Fanget, M. Bretou, E. Karatekin, S. Arbault, M. Guille, F. Darchen, F. Lemaître, C. Amatore, *Angewandte Chemie-International Edition* **2011**, *50*, 5081-5084.
- [24] P. J. O'Connell, X. B. Wang, M. Leon-Ponte, C. Griffiths, S. C. Pingle, G. P. Ahern, *Blood* **2006**, *107*, 1010-1017.
- [25] M. L. Heuze, O. Collin, E. Terriac, A.-M. Lennon-Dumenil, M. Piel, *Methods in molecular biology (Clifton, N.J.)* **2011**, *769*, 415-434.
- [26] G. Faure-Andre, P. Vargas, M.-I. Yuseff, M. Heuze, J. Diaz, D. Lankar, V. Steri, J. Manry, S. Hugues, F. Vascotto, J. Boulanger, G. Raposo, M.-R. Bono, M. Roseblatt, M. Piel, A.-M. Lennon-Dumenil, *Science* **2008**, *322*, 1705-1710.
- [27] T. Mueller, T. Duerk, B. Blumenthal, M. Grimm, S. Cicko, E. Panther, S. Sorichter, Y. Herouy, F. Di Virgilio, D. Ferrari, J. Norgauer, M. Idzko, *PLoS One* **2009**, *4*.
- [28] R. Pacheco, C. E. Prado, M. J. Barrientos, S. Bernales, *Journal of Neuroimmunology* **2009**, *216*, 8-19.
- [29] C. Prado, F. Contreras, H. Gonzalez, P. Diaz, D. Elgueta, M. Barrientos, A. A. Herrada, A. Lladser, S. Bernales, R. Pacheco, *J. Immunol.* **2012**, *188*, 3062-3070.
- [30] K. Nakano, T. Higashi, R. Takagi, K. Hashimoto, Y. Tanaka, S. Matsushita, *International Immunology* **2009**, *21*, 645-654.
- [31] S. Axelsson, R. Elofsson, B. Falck, S. Sjoborg, *Acta Dermato-Venereologica* **1978**, *58*, 31-35.
- [32] A. Meunier, M. Bretou, F. Darchen, M. Guille Collignon, F. Lemaître, C. Amatore, *Electrochimica Acta* **2014**, *126*, 74-80.
- [33] C. Amatore, S. Arbault, Y. Chen, C. Crozatier, F. Lemaître, Y. Verchier, *Angewandte Chemie-International Edition* **2006**, *45*, 4000-4003.
- [34] C. Amatore, J. Delacotte, M. Guille-Collignon, F. Lemaître, *Analyst* **2015**, *140*, 3687-3695.

G-C. thanks "Emergences Ville de Paris 2014" Grant and Institut Universitaire de France Fellowship Program. XL thanks the China Scholarship Council for her financial support with a Ph. D. grant.